

**Heat conduction in driven Frenkel-Kontorova lattices: Thermal pumping and resonance**Bao-quan Ai (艾保全),<sup>1,2</sup> Dahai He (贺达海),<sup>1,\*</sup> and Bambi Hu (胡斑比)<sup>1,3</sup><sup>1</sup>*Department of Physics, Centre for Nonlinear Studies, and the Beijing-Hong Kong-Singapore Joint Centre for Nonlinear and Complex Systems (Hong Kong), Hong Kong Baptist University, Kowloon Tong, Hong Kong, China*<sup>2</sup>*Laboratory of Quantum Information Technology, ICMP and SPTE, South China Normal University, Guangzhou, China*<sup>3</sup>*Department of Physics, University of Houston, Houston, Texas 77204-5005, USA*

(Received 3 November 2009; revised manuscript received 7 March 2010; published 25 March 2010)

Heat conduction through the Frenkel-Kontorova chain under the influence of an ac driving force applied locally at one boundary is studied by nonequilibrium molecular dynamics simulations. We observe the occurrence of thermal resonance, namely, there exists a value of the driving frequency at which the heat flux takes its maximum value. The resonance frequency is determined by the dynamical parameters of the model, which has been numerically explored. Remarkably, the heat can be pumped from the low-temperature heat bath to the high temperature one by suitably adjusting the frequency of the ac driving force. By examining effects of the driving amplitude on heat conduction, we show that the amplitude threshold for nonlinear supratransmission is absent when the system is in contact with heat baths, namely, the heat flux smoothly increases with the increasing of amplitude.

DOI: [10.1103/PhysRevE.81.031124](https://doi.org/10.1103/PhysRevE.81.031124)

PACS number(s): 05.40.-a, 07.20.Pe, 05.90.+m, 44.90.+c

**I. INTRODUCTION**

Theoretical studies of heat conduction in low-dimensional system in recent years have enriched our understanding of the familiar macroscopic phenomenon from a microscopic point of view [1,2]. Recurrent theoretical interest in this field partly lies in the rapid progress in probing and manipulating thermal properties of nanoscale systems, which unveils the possibility of designing thermal devices with optimized performance at the atomic scale. As we all know, devices that control the transport of electrons, such as the electrical diode and transistor, have been extensively studied and led to the widespread applications in modern electronics. However, it is far less studied for their thermal counterparts as to control the transport of phonons (heat flux), possibly by reason that phonons are more difficult to control than electrons. From the theoretical point of view, the difficulty may first lie in quasiparticle entity of the phonon, leading to the failure to characterize the dynamical motion in the real space. A second difficulty consists in the lack of general principles of nonequilibrium statistical mechanics currently, which is nevertheless required to understand the phonon transport through a system in the presence of a temperature gradient. Recently, it has been revealed by theoretical studies in model systems that, such as electrons and photons, phonons can also perform interesting function [3], which shed light on the possible designs of thermal devices. For example, heat conduction in asymmetric nonlinear lattices demonstrates rectification phenomenon, namely, the heat flux can flow preferably in a certain direction [4–11]. Remarkably, a thermal rectifier has been experimentally realized by using gradual mass-loaded carbon and boron nitride nanotubes [12]. Furthermore, Li, Wang, and Casati have proposed a theoretical model of the thermal transistor [13], for which an interesting property called negative differential thermal resistance plays

a crucial role. In addition, it has been demonstrated how to make thermal logic gates and thermal memory for possible use in future phononic computers [14,15]. Nevertheless, it is clear that further studies are necessary to understand the mechanism of phonon transport as to design possible thermal devices. One interesting example of these devices is the heat pump, for which a microscopic model is proposed in this study.

From the second law of thermodynamics, one can know that heat cannot spontaneously flow from objects of lower temperature to that of higher temperature. Directing of heat against the temperature bias requires the application of external work on the system. Recently, a quantum model for a heat pump has been proposed, which consists of a molecular unit connecting to two heat baths with different temperature [16]. By applying an external modulation of the energy levels of the molecular, the energy can be transported from a cold to a hot reservoir. Similar models are proposed as the stochastic effect of the energy level is taken into account [17,18]. Li *et al.* have shown that the heat flux can be directed against the thermal bias in nonlinear lattice models as the temperature of a heat bath is time-periodically modulated [19]. Obviously, novel designs of a microscopic heat pump based on different mechanisms are desirable. As mentioned above, the application of an external perturbation is necessary for the system to operate as a heat pump. A natural option for the external perturbation is the time-periodical driving force as to do work on the system. Energy propagation in nonlinear models driven by a time-periodical force has been extensively studied in recent years [20–24]. These studies mainly focus on effects of the amplitude of the driving force on energy transport through the driven deterministic system. An interesting phenomenon called *nonlinear supratransmission* [20] may occur in these systems, namely, the energy transmission in the forbidden gap become possible when the amplitude of driving force is larger than a critical threshold.

In the present study, we study heat conduction through the Frenkel-Kontorova (FK) chain by applying a sustained sinu-

\*dhhe@hkbu.edu.hk

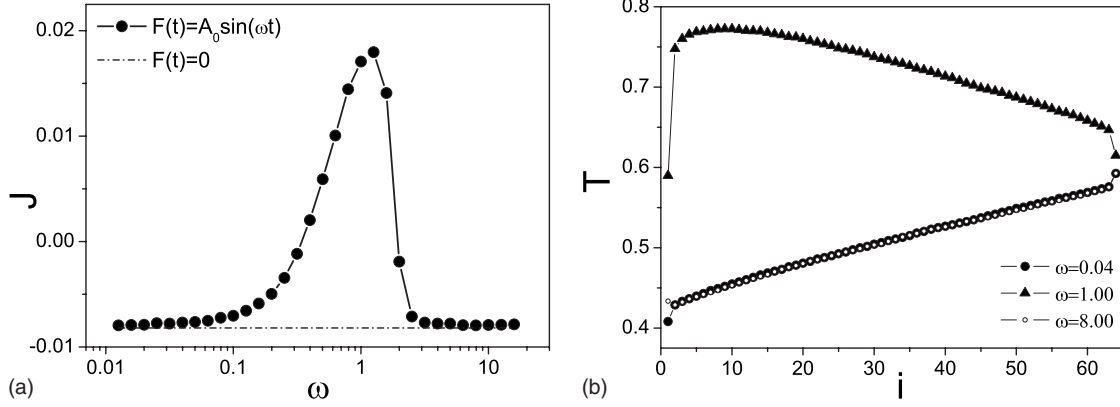


FIG. 1. (a) Heat flux  $J$  as a function of the driving frequency  $\omega$  for  $T_- = 0.4$ ,  $T_+ = 0.6$ ,  $V = 5.0$ ,  $k = 1.0$ ,  $A_0 = 1.0$ , and  $N = 64$ . The dashed line denotes the heat flux for the nondriving case. (b) The temperature profiles for different values of frequencies  $\omega = 0.04$ ,  $1.0$ , and  $8.0$ , respectively.

soidal force at one end of the chain. The difference between the previous deterministic model [20] and the present model is that our system is put in contact with two heat baths at different temperature and the transport process is thus stochastic. We will see that in the presence of the noise, the amplitude threshold for nonlinear supratransmission vanishes. As the effect of the frequency of the driving force is concerned, which is less studied previously, we observe that thermal resonance occurs at a given driving frequency. The effect of the dynamical parameters on the resonance frequency is numerically investigated. Especially, it is interesting to find that heat can be transported against the temperature bias by suitably adjusting the frequency of the driving force, which might have feasible applications.

## II. MODEL AND METHODS

We consider the FK chain, which is a well studied nonlinear model for heat conduction [1]. A sustained time-periodical force is applied at one end of the FK chain, that is, on the first particle we impose the force  $F(t)$ . The Hamiltonian of the whole system is

$$H = \sum_i \frac{p_i^2}{2m} + \frac{1}{2}k(x_i - x_{i+1} - a)^2 - \frac{V}{(2\pi)^2} \cos(2\pi x_i) - \delta_{1,i} x_i F(t), \quad (1)$$

where  $x_i$  and  $p_i$  denotes the position and momenta of particles.  $m$  is the mass of the particle,  $k$  the coupling constant,  $a$  the equilibrium distance of the particles,  $V$  the amplitude of the on-site potential, and  $\delta$  is the Dirac delta function. The external driving force on the first particle is

$$F(t) = A_0 \sin(\omega t), \quad (2)$$

where  $A_0$  is the amplitude of the external force and  $\omega$  is its frequency.

As to obtain a stationary heat flux, the chain is connected to two heat baths at temperature  $T_+$  and  $T_-$ , receptively. Fixed boundary conditions are taken, i.e.,  $x_0 = x_{N+1} = 0$ . The equations of motion for the central particles ( $i = 2, 3, \dots, N-1$ ) are

$$m\ddot{x}_i = -\frac{V}{2\pi} \sin(2\pi x_i) + k(x_{i+1} + x_{i-1} - 2x_i). \quad (3)$$

The heat baths are simulated in our study by Langevin reservoirs, for which the equations of motion for boundary particles ( $i = 1, N$ ) are given by

$$m\ddot{x}_1 = -\frac{V}{2\pi} \sin(2\pi x_1) + k(x_2 - 2x_1) + A_0 \sin(\omega t) - \gamma \dot{x}_1 + \xi_-(t), \quad (4)$$

$$m\ddot{x}_N = -\frac{V}{2\pi} \sin(2\pi x_N) + k(x_{N-1} - 2x_N) - \gamma \dot{x}_N + \xi_+(t), \quad (5)$$

where  $\gamma$  is the friction coefficient and the noise terms  $\xi_{\pm}$  satisfy the fluctuation dissipation relations  $\langle \xi_-(t) \xi_-(t') \rangle = 2\gamma k_B T_- \delta(t-t')$ ,  $\langle \xi_+(t) \xi_+(t') \rangle = 2\gamma k_B T_+ \delta(t-t')$ ,  $k_B$  being Boltzmann's constant. The dot stands for the derivative with respect to time  $t$ .

In our simulations, for simplicity we set the mass of the particles, the equilibrium distance and friction coefficient  $m = a = \gamma = 1$ . The local heat flux is defined as  $J_i(t) = k \langle \dot{x}_i(x_i - x_{i-1}) \rangle$  and the local temperature is  $T_i = \langle m \dot{x}_i^2 \rangle$ .  $\langle \dots \rangle$  denotes an ensemble average over time. The average heat flux  $J$  over the driving period is  $J = \frac{\omega}{2\pi} \int_0^{2\pi/\omega} J_i(t) dt$ , which is equal to the long-time average. The equations of motion are integrated by using a second-order Stochastic Runge-Kutta algorithm [25] with a small time step  $h = 0.005$ . The simulations are performed long enough to allow the system to reach a nonequilibrium steady state in which the local heat flux is constant along the chain. To obtain a steady state, the total integration is typically  $10^{10}$  time units. We have checked that this is sufficient for the system to reach a steady state since the time-averaged heat flux is independent of the site.

## III. NUMERICAL RESULTS AND DISCUSSION

Figure 1(a) shows the heat flux  $J$  as a function of driving frequency  $\omega$  with  $T_- = 0.4$  and  $T_+ = 0.6$ . Since  $T_- < T_+$ , the heat flux will flow from site  $i = N$  to site  $i = 1$  (negative sign

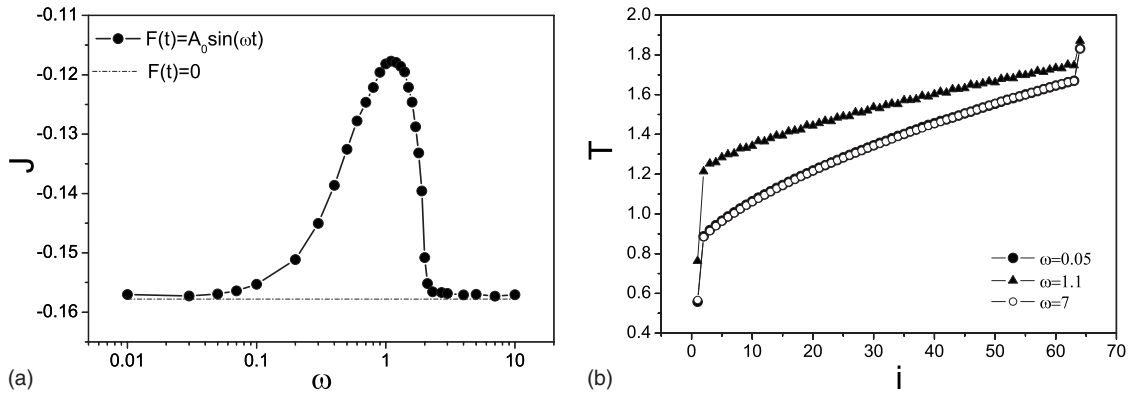


FIG. 2. (a) Heat flux  $J$  as a function of the driving frequency  $\omega$ . Except for  $T_+ = 2$ , all the other parameters are the same as those for Fig. 1. The dashed line denotes the heat flux for the nondriving case. (b) The temperature profiles for different values of frequencies  $\omega = 0.05$ , 1.1, and 7.0, respectively.

for the convention) if the external driving force is absent. However, the situation is changed if the ac driving force acts on the first particle. From Fig. 1(a), we can see that the heat flux increases at first and then decreases as the driving frequency  $\omega$  increases. There exists a value of the driving frequency  $\omega = \omega_m$  at which the heat flux takes its maximum value  $J_m$ , indicating the presence of thermal resonance at  $\omega = \omega_m$ . The cooperation between the intrinsic response time of the system and the external driving frequency leads to the occurring of thermal resonance. In the adiabatic limit  $\omega \rightarrow 0$ , the external force can be expressed by two opposite static forces, yielding the driving force  $F = \frac{1}{2}[A_0 + (-A_0)]$ , so the effects of the external driving force disappear and the current tends to a value  $J_0$  corresponding to the case without the external force. When the external force oscillates very fast at  $\omega \rightarrow \infty$ , the first particle will experience a time averaged constant force  $F = \int_0^{2\pi/\omega} F(t) dt = 0$  and the other particles cannot respond timely to the changing of the force, so the effects of the external force vanishes and the current tends also to that for the nondriving case. Remarkably, the heat flux crosses zero and becomes positive at some intermediate regime of the frequency, which means that the direction of the heat flux is reversed. Consequently, the system can operate as a heat pump to transfer heat from the low temperature heat bath to the high one by suitably adjusting the frequency of the external force.

In order to understand the pumping effect, we also study the temperature profile for different values of the frequency  $\omega$ . The results are depicted in Fig. 1(b). The temperature profiles for both slow ( $\omega = 0.04$ ) and fast ( $\omega = 8.0$ ) driving forces are nearly the same as that of the nondriving case. In other words, force at both adiabatic limit and fast-driving limit cannot change the temperature profiles. In clear contrast to a nondriving case, the temperature profile for a suitable frequency  $\omega = 1.0$  exhibits an opposite temperature gradient, thus indicating the reversal of the heat flux.

As shown in Fig. 2(a), both the magnitude of heat current  $J_0$  for the nondriving case and the resonant heat flux  $J_R = |J_m - J_0|$  increases when the temperature difference increases. As the temperature difference is large enough,  $|J_0|$  will be larger than  $J_R$ . Therefore, the sign of the heat flux persists the same as  $J_0$  when one adjusts the driving fre-

quency, i.e., the pumping effect will disappear. One can also see that from Fig. 2(b), in which the sign of the temperature gradient for  $\omega = \omega_m = 1.1$  is the same as that for the low ( $\omega = 0.05$ ) and high frequency ( $\omega = 7$ ) limit. However, one should note that there still exists thermal resonance. The change in the resonant frequency  $\omega_m$  is slight as the temperature difference increases, showing that the resonant frequency is an intrinsic quantity of the system.

We further investigate the effect of the driving amplitude on heat conduction in the given system, as shown in Fig. 3. One can find in Fig. 3(a) that the higher driving amplitude consistently yields the larger magnitude of the heat flux. Thus, the reversal effect of the heat flux cannot occur when the driving amplitude is low enough. Note that the resonance frequency is independent of the driving amplitude, which shows that the resonance frequency is an intrinsic property of the system. Figure 3(b) depicts the maximum heat flux  $J_m$  obtained at  $\omega = \omega_m$  as a function of the driving amplitude. We can see that  $J_m$  increases with the increasing of the driving amplitude by a power-law behavior  $J_m \propto A_0^\alpha$ , where  $\alpha = 2.30$  for our system. One should note that  $J_m$  is proportional to the square of the driving amplitude ( $\alpha = 2$ ) for a pure harmonic chain in the absence of the heat baths [21]. The deviation of the power from  $\alpha = 2$  for the FK chain is due to the interplay of the nonlinearity and noise in the model. As mentioned above, in the absence of the heat baths, there exists a threshold of the driving amplitude  $A_c$  [20–24], above which energy can be transported through the system when the driving frequency is in the forbidden band gap ( $\omega < \sqrt{V}$  or  $\omega > \sqrt{4k + V}$ ). However, one can see from Fig. 3(c) that heat flux smoothly increases as the driving amplitude increases from zero, even though the driving frequency is in the forbidden band gap. The absence of the threshold can be understood in the following. The existence of the threshold lies in the existence of the spatially localized breather [20]. The energy is triggered to be transmitted when the oscillation amplitude of the static breather is too small to match the force amplitude  $A_0$  as  $A_0$  increases. Nevertheless, the system cannot adjust a perfect static breather due to the presence of the noise. The deformation of the breather leads to the occurring of nonlinear supratransmission for any values of the force amplitude.

We next investigate numerically the role of the coupling constant on thermal resonance. The results are shown in

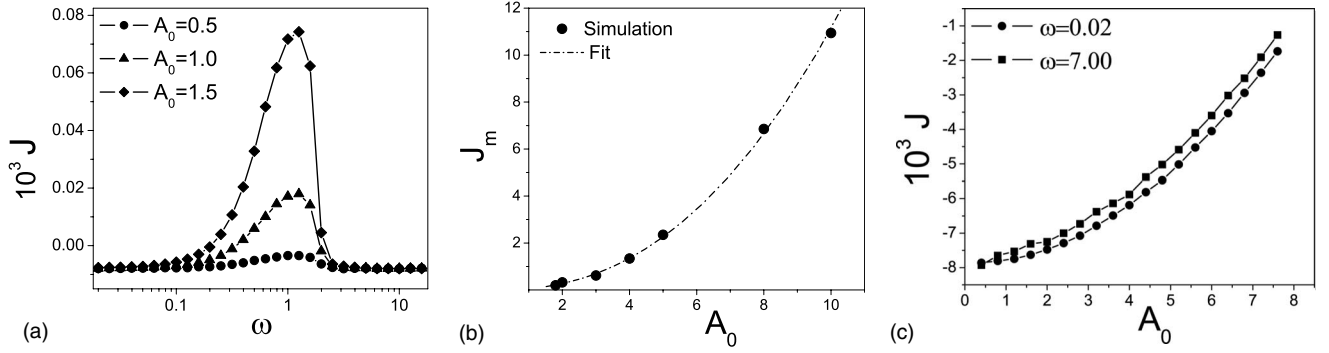


FIG. 3. (a) Heat flux  $J$  as a function of driving frequency  $\omega$  for different driving amplitudes  $A_0=0.5, 1.0,$  and  $1.5$ . Solid lines are drawn to guide the eye. (b) The maximum heat flux  $J_m$  versus the amplitude  $A_0$ . The solid circle denotes the simulation result while the dotted line corresponds a fit  $J_m \propto A_0^{2.30}$ . (c) The heat flux as a function of  $A_0$  as the driving frequency is in the forbidden band gap, e.g.,  $\omega=0.02$  and  $\omega=7$ . For plots (a)–(c), the parameters are set as  $T_- = 0.4$ ,  $T_+ = 0.6$ ,  $V = 5.0$ ,  $k = 1.0$ , and  $N = 64$ .

Figs. 4(a) and 4(b). The height of the peak flux, mainly contributed from the driving force, increases as the coupling constant increases. Remarkably, the position of the peak shift to high-frequency region as the coupling constant increases, showing that the characteristic response time of the system is decreased. From Fig. 4(b) we find that the resonance frequency  $\omega_m$  increases with the coupling constant by a power law  $\omega_m \propto k^\gamma$ , for which fitting result gives  $\gamma=0.66$ .

To gain additional insight of thermal resonance, we also explore the effect of the nonlinear on-site potential on heat conduction. One can see from Fig. 5 that the resonance peak decreases as the height of the on-site potential increases. Obviously, for a very high on-site potential it is very difficult to transfer heat from one heat bath to another. When the on-site potential, in competition with the thermal energy of the system, cannot be neglected, the particles are confined in the valley of the on-site potential, which vary the response time of the chain. A direct result is a shift of the phonon band to high frequency region as the height of the on-site potential increases. Therefore, one can see from Fig. 5(b) that the resonance frequency increases with the increasing of  $V$ .

Figure 6 shows the size effect of thermal resonance phenomena. The total heat flux increases to a saturation value when the system size increases since the thermal conductiv-

ity of the FK model is finite in the thermodynamic limit [26]. Thermal resonance effect does not disappear as the system size varies. This means that occurring of thermal resonance and hence the thermal pumping is not a small-size effect, which is crucial for possible practical application as to control the heat flux. Remarkably, the resonance frequency is independent of the system size. This is different with the results in Ref. [19], which shows that a characteristic frequency will be shifted by varying the system size. The difference lies in the different response of the system to the mechanical modulation and the thermodynamic modulation.

#### IV. CONCLUDING REMARKS

In conclusion, we study heat conduction through the FK chain in the presence of an ac driving force applied at one end of the chain. The ac driving force provides another source of energy flow, by which a controllable manipulation of the heat flow can be readily achieved. It is found that there exists a certain value of the driving frequency at which the heat flux takes its maximum, indicating the occurrence of thermal resonance. The effects of the external driving force come to vanish in both the adiabatic limit and the fast-driving limit. We also show that the amplitude threshold for

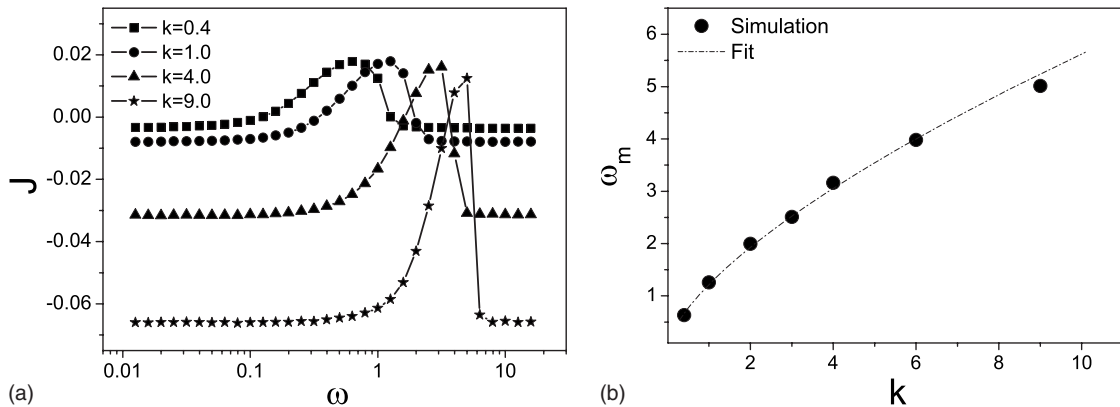


FIG. 4. (a) Heat flux  $J$  as a function of driving frequency  $\omega$  for different values of coupling constant  $k=0.4, 1.0, 4.0,$  and  $9.0$ . Solid lines are drawn to guide the eye. (b) Resonant frequency  $\omega_m$  versus the coupling constant  $k$ . The solid circle denotes the simulation result and the dotted line corresponds a fit proportional to  $k^{0.66}$ . For both (a) and (b),  $T_- = 0.4$ ,  $T_+ = 0.6$ ,  $V = 5.0$ ,  $A_0 = 1.0$ , and  $N = 64$ .



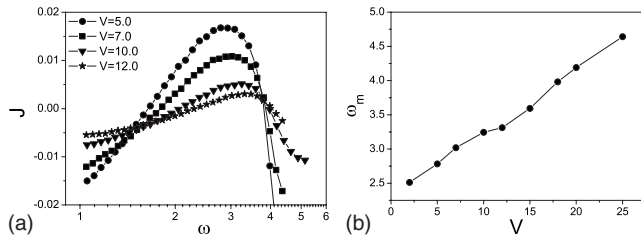


FIG. 5. (a) Heat flux  $J$  versus driving frequency  $\omega$  for different height of the on-site potential  $V=5.0, 7.0, 10.0,$  and  $12.0$ . Here  $T_- = 0.4, T_+ = 0.6, k = 4.0, A_0 = 1.0,$  and  $N = 64$ . (b) The resonance frequency  $\omega_m$  as a function of the height  $V$  of the on-site potential.

the nonlinear supratransmission vanishes in our model due to the presence of the noise. This means that driving force of small amplitude can contribute to heat conduction through the driving frequency is in the forbidden band gap. Thermal resonance occurs when the driving frequency cooperates with the response time of the system. The intrinsic resonance frequency is determined by the dynamical parameters of the model, such as the coupling constant and the strength of the on-site potential, and independent of the system size. However, a rigorous exact analysis to characterize the response time of the system and thus the resonance frequency is so far unavailable, which deserves further investigations.

As far as the possible design of thermal devices is concerned, we propose a model of the heat pump, where the heat flux can be directed against the temperature bias by suitably tailoring the frequency of the ac driving force. This is very similar to the Brownian particle pump [27,28] in which the particles can be pumped through the system from a reservoir at low concentration to one at the same or higher concentration by zero mean external forces. Although we here focus on the FK model, we have found similar results also for other models, such as the  $\phi^4$  model [1], the coupled-rotor model [29] and the Fermi-Pasta-Ulam model [30]. This indicates that all of these coupled-oscillator systems (with Fourier or non-Fourier behavior), have their own intrinsic response time, which is critical for the occurrence of thermal resonance. Note that the occurrence of the pumping effect depends on system parameters, e.g., the temperature difference. As large temperature difference is applied on the sys-

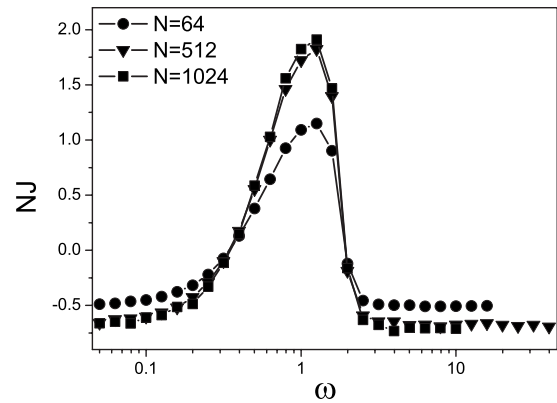


FIG. 6. The total heat flux  $N \times J$  versus the driving frequency  $\omega$  for different lattice sizes  $N=64, 512,$  and  $1024$ . Here  $V=5.0, T_- = 0.4, T_+ = 0.6, k = 1.0,$  and  $A_0 = 1.0$ .

tem, e.g., the  $\phi^4$  model [31,32], the direction of the heat flux will not be reversed since the resulted resonant heat flux is too small in comparison with the heat current for the non-driving case.

Practically, the presented model design of the heat pump would be feasible to realize in laboratory since the ac driving force can be readily prepared in many ways from mechanics, optics, magnetics, etc. Another feasibility lies in the size-independent property of thermal resonance effect. Therefore, further developments with respect to thermal resonance and pumping in various physical systems such as magnetic thin films [33], Josephson junction arrays [34], and granular systems [35] would be interestingly expected.

#### ACKNOWLEDGMENTS

We would like to thank members of the Centre for Non-linear Studies for useful discussions. This work was supported in part by grants from the Hong Kong Research Grants Council (RGC) and the Hong Kong Baptist University Faculty Research Grant (FRG). B.A. acknowledges the support of National Natural Science Foundation of China with Grant No. 30600122 and GuangDong Provincial Natural Science Foundation with Grant No. 06025073.

[1] S. Lepri, R. Livi, and A. Politi, *Phys. Rep.* **377**, 1 (2003).  
 [2] A. Dhar, *Adv. Phys.* **57**, 457 (2008).  
 [3] G. Casati, *Nat. Nanotechnol.* **2**, 23 (2007).  
 [4] M. Terraneo, M. Peyrard, and G. Casati, *Phys. Rev. Lett.* **88**, 094302 (2002).  
 [5] D. Segal and A. Nitzan, *Phys. Rev. Lett.* **94**, 034301 (2005).  
 [6] B. Li, L. Wang, and G. Casati, *Phys. Rev. Lett.* **93**, 184301 (2004).  
 [7] N. Yang, N. Li, L. Wang, and B. Li, *Phys. Rev. B* **76**, 020301(R) (2007).  
 [8] B. Hu and L. Yang, *Chaos* **15**, 015119 (2005).  
 [9] B. Hu, D. He, L. Yang, and Y. Zhang, *Phys. Rev. E* **74**,

060101(R) (2006).  
 [10] B. Hu, D. He, L. Yang, and Y. Zhang, *Phys. Rev. E* **74**, 060201(R) (2006).  
 [11] B. Hu, L. Yang, and Y. Zhang, *Phys. Rev. Lett.* **97**, 124302 (2006).  
 [12] C. W. Chang, D. Okawa, A. Majumda, and A. Zettl, *Science* **314**, 1121 (2006).  
 [13] B. Li, L. Wang, and G. Casati, *Appl. Phys. Lett.* **88**, 143501 (2006).  
 [14] L. Wang and B. Li, *Phys. Rev. Lett.* **99**, 177208 (2007).  
 [15] L. Wang and B. Li, *Phys. Rev. Lett.* **101**, 267203 (2008).  
 [16] D. Segal and A. Nitzan, *Phys. Rev. E* **73**, 026109 (2006).

- [17] D. Segal, Phys. Rev. Lett. **101**, 260601 (2008).
- [18] D. Segal, J. Chem. Phys. **130**, 134510 (2009).
- [19] N. Li, P. Hanggi, and B. Li, Europhys. Lett. **84**, 40009 (2008); N. Li, F. Zhan, P. Hanggi, and B. Li, Phys. Rev. E **80**, 011125 (2009).
- [20] F. Geniet and J. Leon, Phys. Rev. Lett. **89**, 134102 (2002).
- [21] R. Khomeriki, S. Lepri, and S. Ruffo, Phys. Rev. E **70**, 066626 (2004).
- [22] P. Maniadis, G. Kopidakis, and S. Aubry, Physica D **216**, 121 (2006).
- [23] T. Dauxois, R. Khomeriki, and S. Ruffo, Eur. Phys. J. Spec. Top. **147**, 3 (2007) and references therein.
- [24] M. Johansson, G. Kopidakis, S. Lepri, and S. Aubry, Europhys. Lett. **86**, 10009 (2009).
- [25] R. L. Honeycutt, Phys. Rev. A **45**, 600 (1992).
- [26] B. Hu, B. Li, and H. Zhao, Phys. Rev. E **57**, 2992 (1998).
- [27] J. M. Sancho and A. Gomez-Marin, Proc. SPIE **6602**, 66020B (2007); A. Gomez-Marin and J. M. Sancho, Phys. Rev. E **77**, 031108 (2008).
- [28] B. Q. Ai and L. G. Liu, J. Chem. Phys. **128**, 024706 (2008); vB. Q. Ai and L. G. Liu, J. Phys. Chem. B **112**, 9540 (2008).
- [29] C. Giardina, R. Livi, A. Politi, and M. Vassalli, Phys. Rev. Lett. **84**, 2144 (2000); O. V. Gendelman and A. V. Savin, *ibid.* **84**, 2381 (2000).
- [30] E. Fermi, J. Pasta, and S. Ulam, in *Collected Paper* edited by E. Fermi (University of Chicago Press, Chicago, 1976), 2, 78.
- [31] K. Aoki and D. Kusnezov, Phys. Lett. A **265**, 250 (2000).
- [32] J. Bricmont and A. Kupiainen, Commun. Math. Phys. **274**, 555 (2007).
- [33] R. Khomeriki, J. Leon, and M. Manna, Phys. Rev. B **74**, 094414 (2006).
- [34] D. Chevriaux, R. Khomeriki, and J. Leon, Phys. Rev. B **73**, 214516 (2006).
- [35] V. Tournat, V. E. Gusev, and B. Castagnède, Phys. Rev. E **70**, 056603 (2004).